ADVANCED ELECTRONIC MATERIALS
www.advelectronicmat.de

Vapor-Coated Monofilament Fibers for Embroidered Electrochemical Transistor Arrays on Fabrics

*Lushuai Zhang and Trisha Andrew**

Fiber-based electrochemical transistors can be embroidered onto fabrics for wearable and implantable bioelectronics. However, the active channel length of known fiber-based electrochemical transistors is defined by the dynamic contact area between the conductive fiber and a liquid electrolyte, meaning that existing iterations cannot be reliably operated upon immersion in biological media. A proof-of-concept parallel-junction electrochemical transistor on a silk fabric with a fixed, micrometer-sized channel length that is independent of electrolyte contact area is reported. A high on/off ratio of 1000, and notable transconductance value of 100 µS at zero gate voltage and low applied drain bias (0.7 V) is obtained, making this device amenable to subsequent incorporation into low-power-consuming integrated circuits. Large-area arrays of this transistor can be rapidly created by straight-stitching a monofilament fiber channel onto a fabric substrate, meaning that simple embroidery approaches can be used to fabricate spatially resolved electrode arrays for electrophysiological applications.

1. Introduction

Depletion-mode organic electrochemical transistors (OECTs) that contain conducting polymer formulations, such as poly(3,4-ethylenedioxythiophene)-poly(styrene sulfonic acid) (PEDOT:PSS), have shown promise in chemical and biological sensing,[1,2] transducer amplification,[3] interfacing with brain cells,[4] and monitoring barrier tissue integrity.[5] Electrically connected arrays of these conducting polymer–based OECTs show superior signal-to-noise ratio for in vivo electrophysiological recording of brain activity compared to traditional metal–electrode arrays.[4,6] Transistor arrays created on soft, biocompatible, organ-conformable substrates would further allow for implantable brain activity monitors and, ultimately, implantable electronics capable of compensating for organ damage.[7] In this sense, fabrics are excellent candidate substrates for implantable OECT arrays, as many examples of surgical fabrics and fabric-like reparative and/or implantable meshes are actively used in modern healthcare.[8]

Dr. L. Zhang, Prof. T. Andrew
Departments of Chemistry and Chemical Engineering
University of Massachusetts Amherst
Amherst, MA 01003, USA
E-mail: tandrew@umass.edu

The ORCID identification number(s) for the author(s) of this article can be found under https://doi.org/10.1002/aelm.201800271.

DOI: 10.1002/aelm.201800271

Conductive fiber–based OECTs, in which a single conductive fiber simultaneously serves as the source/drain electrode and the bias-responsive channel, are perfectly suited for seamless integration into fabrics. Innovative device integration schemes to create woven or knit logic gates, actuators, and biosensors have been reported.[9–17] However, in all reported cases, the device geometry and active channel length of fiber-based OECTs is dynamically defined by the overlapping area between the conductive fiber and a liquid/gel electrolyte droplet.[9–17] If the entire conductive fiber is exposed to electrolyte, then the source/drain electrodes are not defined and the fiber simply acts as a tortuously long channel. Consequently, current examples of fiber-based OECTs cannot readily maintain their reported transistor performance upon being fully immersed in a biological medium or being interfaced with an organ. To create implantable OECT arrays on fabrics, the active channel length in fiber-based devices needs to be a fixed feature that is insensitive to varying electrolyte–fiber contact. To date, straightforward methods to confine the channel length in fiber-based OECTs and drive the device footprint down to the micrometer-length scale are sparse.

Here, we use vapor-coated nylon monofilament fibers to straight-stitch a fixed-channel-length, fiber-based parallel electrochemical transistor on a silk backing fabric. The channel length of our transistor is confined to the front-exposed surface of the monofilament fiber, which is reduced to the micrometer-length scale by taking advantage of the weave density of the silk backing. The geometry of our transistor, including the channel length and channel-to-gate distance, can readily be controlled by the stitching style and density used during device assembly. Our fiber-based OECT displays a high on/off ratio of 1000, and a notable transconductance value of 100 µS at zero gate voltage and a low drain bias (0.7 V), which is comparable to contemporary devices created on rigid glass substrates using conventional lithographic methods. Large-area arrays can be rapidly created by straight-stitching a monofilament fiber channel onto a fabric substrate, meaning that simple embroidery approaches can be used to fabricate spatially resolved electrode arrays for electrophysiological applications. This is also the first demonstration that reactive vapor deposition (RVD) can produce suitable conductive fibers for depletion-mode OECTs.

2. Results and Discussion

Nylon monofilament fibers were chosen as the fiber substrate because they are flexible, strong, biocompatible, and widely used as suture materials.[18] RVD[19] was used to conformally coat the entire circumference of 100 µm diameter nylon monofilament fibers with a stably doped conducting polymer film (**PEDOT-Cl**). A schematic of the RVD chamber and substrate holder used to coat fibers are shown in **Figure 1**. A 1 mm gap between fiber and substrate holder allowed vaporized reactive species to access all exposed surfaces of the fiber and create a uniform and continuous surface coating. Up to 30 feet of fiber could be coated per deposition cycle, which lasted approximately 20 min for a 300 nm thick coating.

The as-deposited PEDOT-Cl films contained trapped $FeCl_3$, which was removed by a post-deposition rinse in methanol. Figure 1c shows the X-ray photoelectron spectroscopy spectra of a PEDOT-Cl film deposited on a glass slide after immersion in methanol. The disappearance of the Fe 2P peak upon soaking in methanol for 30 min indicated complete removal of $FeCl_3$ from the film. The PEDOT-Cl coating remained highly doped, even after methanol immersion, as evidenced by the presence of a strong near infrared absorbance arising from the doped polaron/bipolaron states of PEDOT-Cl, as well as the relatively

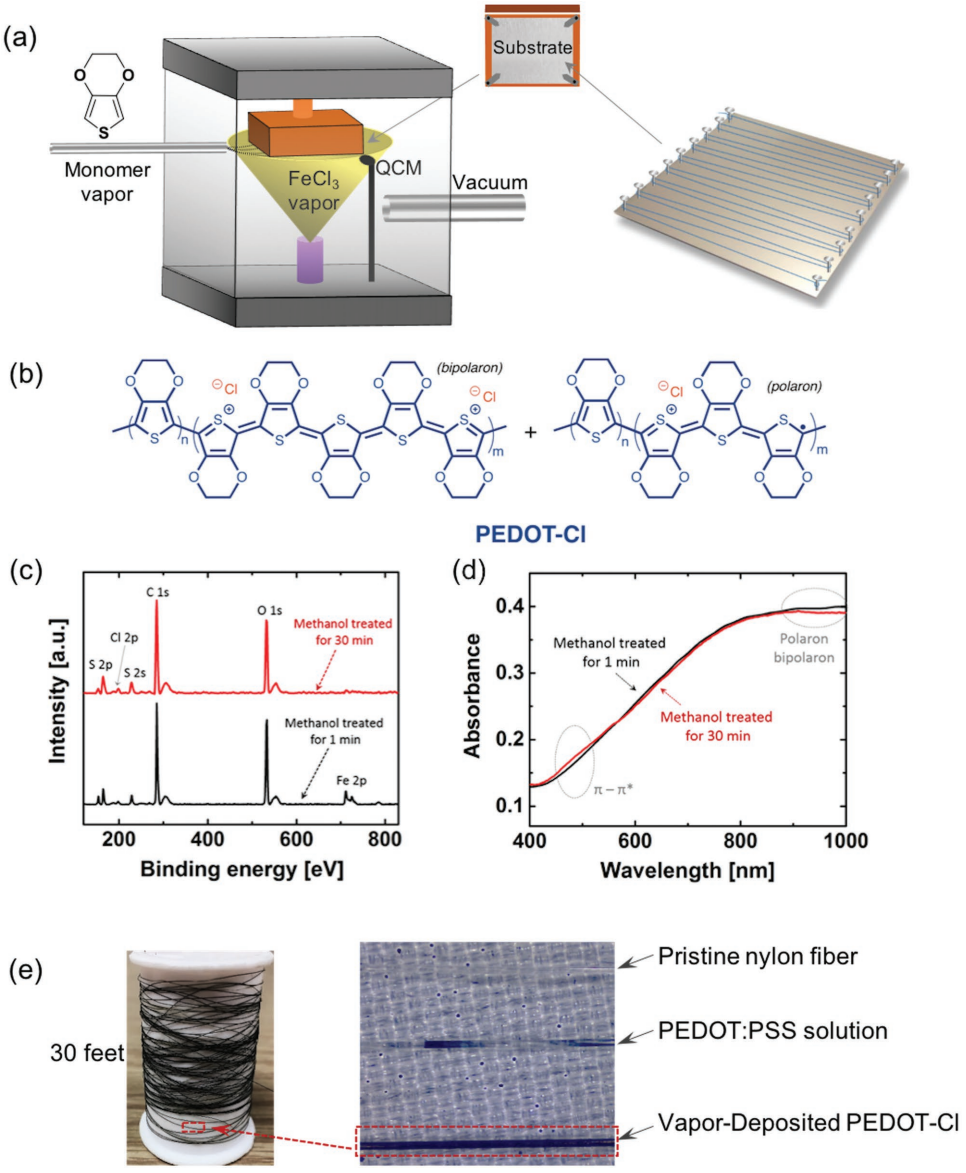

Figure 1. a) Schematic of the reactor and substrate holder used to effect vapor coating of fibers. b) Chemical structure of the conducting PEDOT-Cl polymer coating created on the surface of fibers. c) X-ray photoelectron spectroscopy scans and d) UV–vis absorbance spectra of PEDOT-Cl films after post-deposition rinsing with methanol, showing complete removal of residual iron oxidant. e) (left) Optical image of a 30-foot-long nylon monofilament fiber coated with PEDOT-Cl, and (right) a comparison of the uniformity of the conductive coating obtained using solution processing (dipcoating) and vapor coating.

weak intensity of the π–π^* transition of neutral PEDOT-Cl in the 400–600 nm region.

The optical micrograph in Figure 1e shows a pristine nylon monofilament fiber, a fiber after dipcoating with PEDOT:PSS from a commercial aqueous formulation, and a fiber after vapor-coating with PEDOT-Cl. Coating from solution is highly substrate dependent. Drawing a hydrophobic nylon monofilament fiber through the PEDOT:PSS aqueous solution left behind a nonuniform coating. In stark contrast, uniform coating was obtained by RVD.

The scanning electron microscopy (SEM) and energy-dispersive X-ray spectroscopy (EDX) images in **Figure 2** further revealed the conformal surface coating of PEDOT-Cl on nylon monofilament fibers. The electrically insulating nylon fiber showed severe charging effects, which were mitigated when a uniform, 5 nm thick PEDOT-Cl coating was introduced. A 300 nm thick PEDOT-Cl coating had a slightly rougher surface than that of the 5 nm thick film, though uniform, pinhole-free, conformal coating was still observed. EDX elemental maps for N and S elements affirmed that S was only present on the surface of the Nylon monofilament, meaning that the bulk of the fiber did not contain PEDOT-Cl. This, in turn, meant that the conductive channel of this coated fiber was restricted only to the surface and did not traverse the interior bulk of the fiber, as in previous dipcoated versions of fiber-based OECTs.[9–17] The conductivity of the PEDOT-Cl coated nylon fiber was measured to be 300 S cm^{-1} using a home-built four-point probe station; this value is similar to previously reported figures for prewoven textiles coated with a 300 nm thick layer of PEDOT-Cl.[19b]

There are two known configurations of fiber-based OECTs: a junction OECT[9–15] and parallel OECT.[16,17] In a junction OECT, two fibers coated with conducting polymer are crisscrossed and an electrolyte droplet is added at the dual fiber intersection to complete the device.[9] Such a junction device is susceptible to fiber dislocation by mechanical deformation and the channel length is effectively determined by the surface tension of the electrolyte droplet. Parallel OECTs are easier to fabricate and are more resilient to mechanical deformation. However, the channel length is defined by the size of the electrolyte droplet or micropatterned polydimethylsiloxane reservoirs, leading to channel lengths of several millimeters to centimeters, as well as large device footprints.[11,16,17]

Here, a fixed-channel-length, parallel transistor was created by straight-stitching a surface-coated nylon monofilament fiber onto a hydrophobic silk backing fabric. A summary of our fabrication process is provided in **Figure 3**. A silk fabric was first exposed to 1H,1H,2H,2H-perfluorooctyltriethoxysilane vapor to form a hydrophobic surface. Next, a vapor-coated (300 nm PEDOT-Cl) nylon monofilament fiber was tightly stitched onto the hydrophobic silk fabric, across only one warp/weft thread, thus separating the conductive nylon fiber into three parts: a middle part that was exposed on the front (top) face of the backing textile and served as the bias-responsive transistor channel; and two end parts that were dangling on the back (bottom) face of the backing textile and served as the source and drain electrodes. The dimensions of the exposed middle part of the monofilament fiber were reduced to the micrometer-length scale because of the tight weave density of the backing fabric. A commercial two-ply stainless steel thread was then sewed into the silk textile, in parallel to the nylon fiber, to serve as the gate electrode. A large length of the stainless steel gate thread was deliberately exposed on the front face of the textile substrate to obtain a large gate/channel volume ratio, which has been shown to be optimal for in vivo biosensors and electrophysiological monitors.[20] Nonpolarizable electrodes and small gate/channel volume ratios are best suited for electrochemical logic gates and aqueous-functioning switches.[20] Importantly, the geometry of this device, including the channel length, channel-to-gate distance, and gate/channel volume ratio, can be readily controlled by changing the sewing style and stitching density used during device assembly.

In the final step, liquid electrolyte was introduced onto the front (top) face of the backing textile, covering both the gate electrode and channel. Due to the hydrophobicity of the silk backing textile, the electrolyte automatically formed large droplets on the front (top) surface without soaking through to the back (bottom) surface and interfacing with the two dangling ends of the conductive nylon fiber on the back face. These two dangling ends, therefore, remained unaffected by an applied gate potential and served as stably conductive source/drain electrodes for the front-exposed responsive channel part of the same fiber. Thus, the channel length was

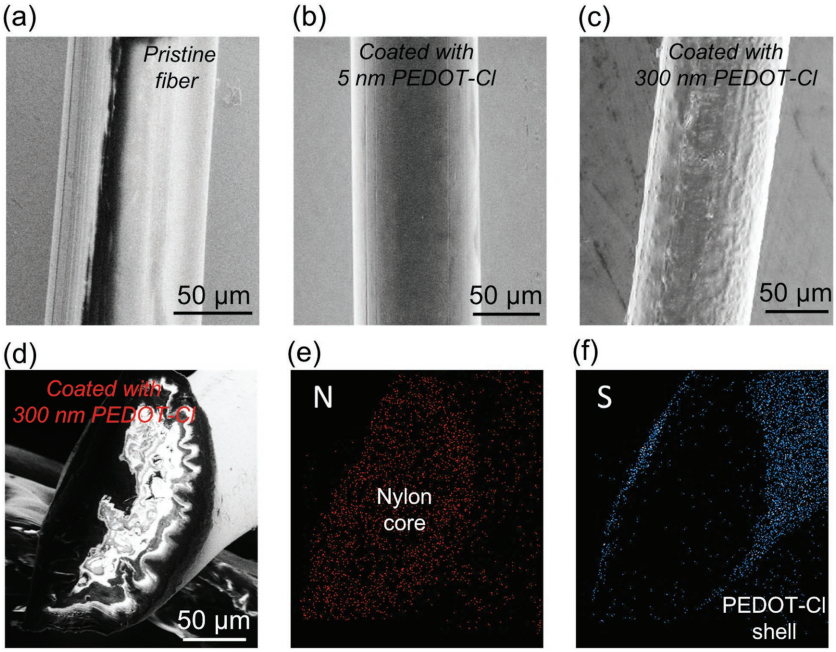

Figure 2. SEM images of a) a pristine nylon monofilament fiber, b) a fiber with a 5 nm-thick PEDOT-Cl coating, and c) a fiber with a 300 nm-thick PEDOT-Cl coating. d) Cross-section SEM image of a nylon fiber with a 300 nm-thick PEDOT-Cl coating. e) EDX mapping of element N and f) element S of the SEM image in (d).

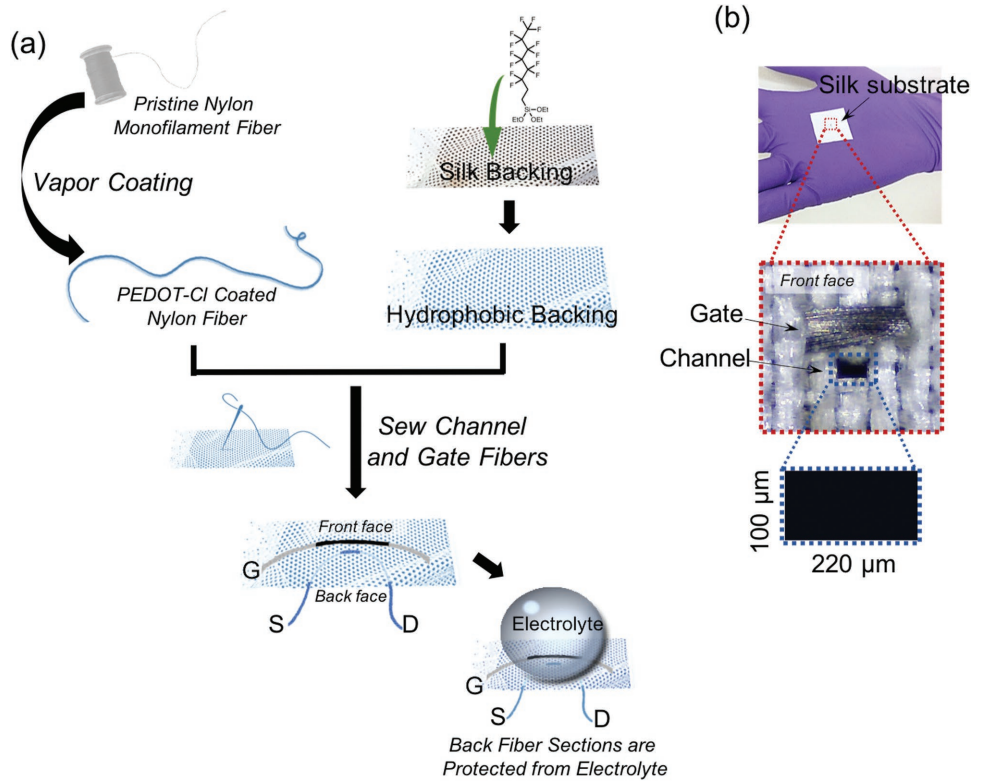

Figure 3. a) Schematic of the process to create a fixed-channel parallel electrochemical transistor on a silk backing. b) Optical image (top) and low-magnification optical micrograph (middle) of a parallel transistor stitched on a textile (shown without electrolyte for clarity).

independent of the electrolyte volume and was only determined by the exposed face of the fiber on the front (top) surface of the textile.

The optical image in Figure 3b shows the front (top) surface of a silk backing fabric with a PEDOT-Cl coated nylon fiber (channel) and a stainless steel thread (gate) sewed on. The little black dot at the center of the red dashed box is the stainless steel thread—the nylon fiber is undiscernible at this scale. Such a device footprint is dramatically miniaturized in comparison to the previously reported parallel OECTs on textiles.[11,16,17] The optical micrograph in the middle of Figure 3b shows that the front-exposed channel length is the same as the width of the warp/weft thread of the silk backing fabric, and that the gate and channel fibers are stitched close together though separated by one warp/weft thread to avoid electrical shorts under mechanical deformation. The high-magnification optical micrograph on the bottom of Figure 3b reveals the exposed channel length to be 220 µm (the fiber diameter was 100 µm).

During operation, the resistance of the front-exposed channel was modulated by the gate electrode, which caused electrochemical dedoping of the PEDOT-Cl surface coating. At null gate potential, PEDOT-Cl was highly doped (oxidized), and behaved as a low-resistance conductor, leading to the "on" state of the OECT. The positive charges on the doped PEDOT-Cl backbone were stabilized by chloride counterions. Upon applying a positive gate potential, PEDOT-Cl was electrochemically reduced (dedoped) to a semiconducting state with high resistance, leading to the "off" state. The chloride anions that were ejected from the film during dedoping migrated toward the gate electrode and formed an electrical double layer across the gate/electrolyte interface.

Device performance metrics are provided in **Figure 4**. The magnitude of the drain current steadily increased with increasing PEDOT-Cl coating thickness (Figure S1, Supporting Information) but remained insensitive to the size/volume of the electrolyte droplet used during measurement. The output characteristics revealed a typical *p*-type depletion-mode transistor, consistent with simulated models,[21] with a linear region at low V_{DS} and a saturation region at high V_{DS}. As gate voltage was increased, the pinch-off point shifted toward a smaller V_{DS}. The linear region was attributed to a uniform charge distribution throughout the channel. Pinch-off occurred as charges depleted (dedoping) near the drain electrode under high V_{DS}. The applied gate voltage facilitated charge depletion near the drain electrode and the device was completely turned off at a gate voltage of 0.9 V. The transfer characteristics revealed an on/off ratio of greater than 1000 for low gate voltages at $V_{DS} = -0.7$ V, making this device amenable to subsequent incorporation into low-power-consuming integrated circuits. A maximum transconductance, $g_m = \Delta I_d/\Delta V_g$, of 110 µS was obtained at zero gate voltage, which is highly sought-after for single-power transducer amplifiers.

Large-area arrays were rapidly created by straight-stitching lines of a monofilament fiber channel followed by a stainless steel gate channel onto a 2 × 2 in. silk backing fabric. After this embroidery, the threads were cut on the back side to electrically isolate each device (**Figure 5**). The output characteristics of each individual parallel transistor after cutting (Figure 5c)

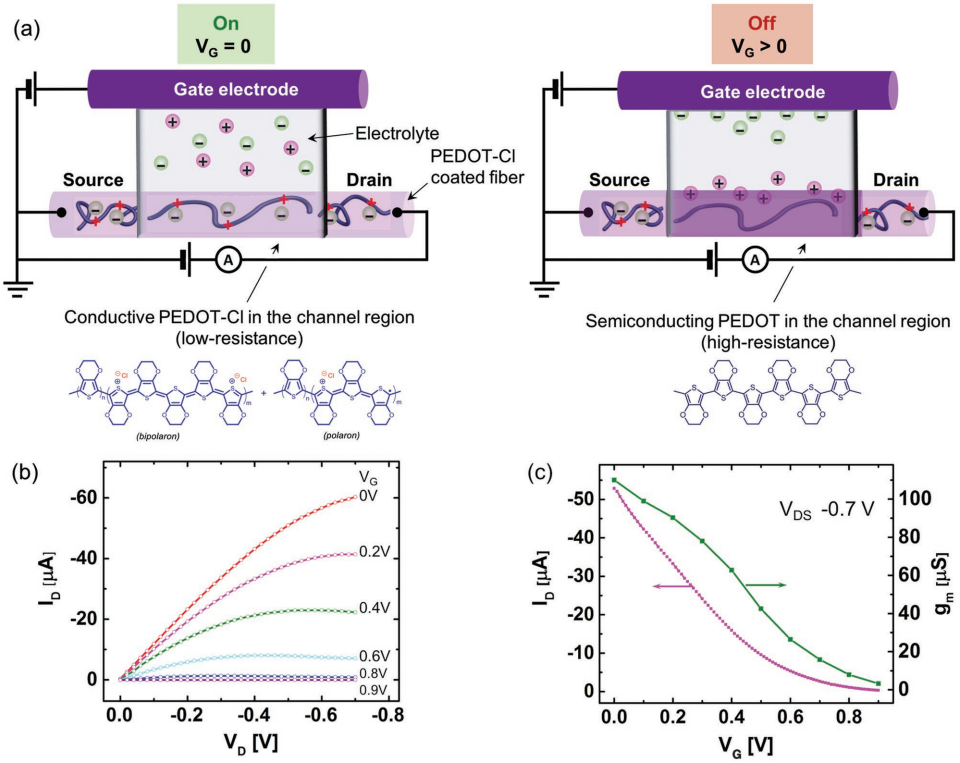

Figure 4. a) Operative mechanism of depletion-mode, parallel-junction electrochemical transistor. b) Output I-V characteristics and c) transfer I-V characteristics of a parallel transistor created using a nylon monofilament fiber vapor coated with 300 nm-thick PEDOT-Cl.

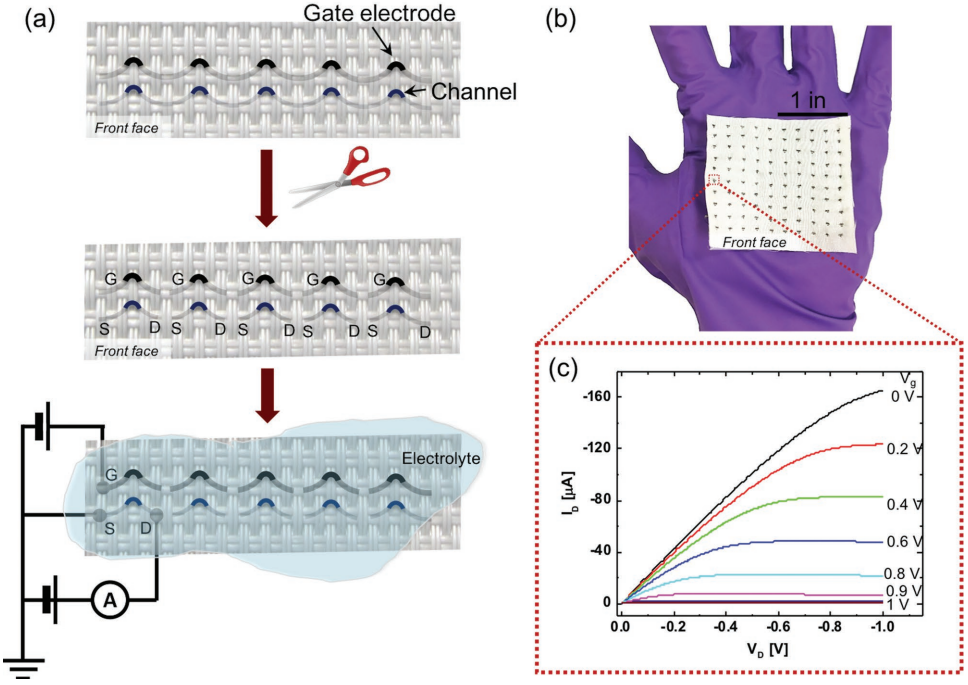

Figure 5. a) Schematic of the process to embroider a parallel electrochemical transistor array on a silk backing. b) Optical image of a parallel electrochemical transistor array on a 2 × 2 in. fabric. c) Output I-V characteristics of one representative, isolated device within the array, recorded by placing the entire front face of the fabric on the meniscus of an aqueous saline solution.

were similar to those of the single device described in Figure 4. Therefore, simple embroidery approaches successfully created spatially resolved electrode arrays, which are integral for electrophysiological monitoring. Further, because of the hydrophobicity of the backing fabric, the effective channel length for each device in this array was not dynamically dependent on the conductive fiber–electrolyte contact area. Therefore, the entire front face of the embroidered transistor array could be covered in a liquid electrolyte solution while the channel current output for each individual device remained invariant.

3. Conclusion

We report a proof-of-concept parallel electrochemical transistor array on a commercial silk textile, where important device parameters, such as channel length and channel-to-gate distance, are automatically defined by the weave density of the backing textile instead of a dynamic electrolyte contact area. The device footprint is significantly smaller than previously reported textile transistors. The current output of these transistor arrays remains invariant when immersed in liquid electrolyte (saline), allowing future interfacing with cells and living tissue. Moreover, to the best of our knowledge, this is the first demonstration of electrochemically gated conductivity (depletion-mode) in a vapor-deposited conjugated polymer film.

OECTs are famously used to interface with cells and/or living tissue, where various biological events modulate the effective gate voltage.[1–6] In these cases, the maximum sensitivity of the transistor to the biological event under study is determined by the device transconductance, $g_m = \Delta I_d/\Delta V_g$, which needs to be maximized when the transistor is operated at a low, constant gate voltage (ideally, null gate voltage). For our device, the maximum transconductance (100 μS) is obtained at zero gate voltage, meaning that these fabric-backed devices can be used for low-power, single-source electrophysiological monitoring.[20] Furthermore, because vapor-deposited conducting polymer films were previously revealed to possess remarkable ionic permselectivity,[22] ion-dependent mechanistic details for a particular biochemical pathway can be systematically probed using our parallel electrochemical transistors.

The fabrication process we describe here also boasts a straightforward path to tune certain device metrics using creative embroidery approaches and tight-woven textiles. For example, the gate voltage for maximum transconductance can be tuned by modifying the channel geometry and gate material. The transfer characteristics are sensitive to the gate material and gate/channel volume ratio. A polarizable gate electrode and a large volume ratio of gate/channel was used in this work because this condition leads to optimized biosensors.[20] Non-polarizable gate electrodes and small volume ratios of gate/channel can also be readily applied for different applications.

4. Experimental Section

Materials and Methods: 3,4-Ethylenedioxythiophene (EDOT) (97%) was purchased from TCI America, and $FeCl_3$ (97%) was purchased from Sigma-Aldrich and used without further purification. Nylon monofilament fibers and silk textiles were used as received. The electrolyte was composed of 33 wt% polystyrene sulfonate, 12 wt% glycol, and 8 wt% sorbitol in deionized water. SEM was performed using a Magellan 400 field-emission microscope. Film thicknesses were measured on a Veeco Dektak 150 profilometer.

Vapor Coating of Nylon Fibers: A detailed procedure for RVD was previously reported.[19] For this work, argon gas was introduced into the chamber via a needle valve to maintain the total chamber pressure at 300 ± 10 mTorr. The substrate stage was maintained at 80 °C. The deposition rate and film thickness were monitored by a quartz crystal microbalance. PEDOT-Cl was deposited on a nylon fiber and a polyethylene terephthalate (PET) film simultaneously. The PEDOT-Cl on PET sample was used to confirm the film thickness. After deposition, the substrate stage was cooled down to 50 °C before samples were removed from the chamber. Samples were rinsed in methanol for up to 30 min under air.

Supporting Information

Supporting Information is available from the Wiley Online Library or from the author.

Acknowledgements

The authors gratefully acknowledge support by the David and Lucile Packard Foundation.

Conflict of Interest

The authors declare no conflict of interest.

Keywords

arrays, monofilaments, organic electrochemical transistors, reactive vapor deposition, sewing

Received: April 26, 2018
Revised: June 1, 2018
Published online: June 28, 2018

[1] X. Strakosas, M. Bongo, R. M. Owens, *J. Appl. Polym. Sci.* **2015**, *132*, 41735.
[2] M. Braendlein, A.-M. Pappa, M. Ferro, A. Lopresti, C. Acquaviva, E. Mamessier, G. G. Malliaras, R. M. Owens, *Adv. Mater.* **2017**, *29*, 1605744.
[3] M. Braendlein, T. Lonjaret, P. Leleux, J.-M. Badier, G. G. Malliaras, *Adv. Sci.* **2017**, *4*, 1600247.
[4] a) D. Khodagholy, T. Doublet, P. Quilichini, M. Gurfinkel, P. Leleux, A. Ghestem, E. Ismailova, T. Hervé, S. Sanaur, C. Bernard, G. G. Malliaras, *Nat. Commun.* **2013**, *4*, 1575; b) W. Lee, D. Kim, N. Matsuhisa, M. Nagase, M. Sekino, G. G. Malliaras, T. Yokota, T. Someya, *Proc. Natl. Acad. Sci.* **2017**, *114*, 10554; c) W. Lee, D. Kim, J. Rivnay, N. Matsuhisa, T. Lonjaret, T. Yokota, H. Yawo, M. Sekino, G. G. Malliaras, T. Someya, *Adv. Mater.* **2016**, *28*, 9722.
[5] L. H. Jimison, S. A. Tria, D. Khodagholy, M. Gurfinkel, E. Lanzarini, A. Hama, G. G. Malliaras, R. M. Owens, *Adv. Mater.* **2012**, *24*, 5919.
[6] J. Rivnay, P. Leleux, M. Ferro, M. Sessolo, A. Williamson, D. A. Koutsouras, D. Khodagholy, M. Ramuz, X. Strakosas,

R. M. Owens, C. Benar, J.-M. Badier, C. Bernard, G. G. Malliaras, *Sci. Adv.* **2015**, *1*, e1400251.

[7] D.-H. Kim, J. Viventi, J. J. Amsden, J. Xiao, L. Vigeland, Y.-S. Kim, J. Blanco, B. Panilaitis, E. S. Frechette, D. Contreras, D. L. Kaplan, F. G. Omenetto, Y. Huang, K.-C. Hwang, M. R. Zakin, B. Litt, J. A. Rogers, *Nat. Mater.* **2010**, *9*, 511.

[8] a) C. Massaroni, P. Saccomandi, E. Schena, *J. Funct. Biomater.* **2015**, *6*, 204; b) G. Li, Y. Li, G. Chen, J. He, Y. Han, X. Wang, D. L. Kaplan, *Adv. Healthcare Mater.* **2015**, *4*, 1134; c) M. Akbari, A. Tamayol, S. Bagherifard, L. Serex, P. Mostafalu, N. Faramarzi, M. H. Mohammadi, A. Khademhosseini, *Adv. Healthcare Mater.* **2016**, *5*, 751; d) B. M. Quandt, L. J. Scherer, L. F. Boesel, M. Wolf, G.-L. Bona, R. M. Rossi, *Adv. Healthcare Mater.* **2015**, *4*, 330; e) M. Papaiordanidou, S. Takamatsu, S. Rezaei-Mazinani, T. Lonjaret, A. Martin, E. Ismailova, *Adv. Healthcare Mater.* **2016**, *5*, 2000.

[9] M. Hamedi, R. Forchheimer, O. Inganas, *Nat. Mater.* **2007**, *6*, 357.

[10] H. M. Kim, H. W. Kang, D. K. Hwang, H. S. Lim, B.-K. Ju, J. A. Lim, *Adv. Funct. Mater.* **2016**, *26*, 2706.

[11] I. Gualandi, M. Marzocchi, A. Achilli, D. Cavedale, A. Bonfiglio, B. Fraboni, *Sci. Rep.* **2016**, *6*, 33637.

[12] C. Muller, M. Hamedi, R. Karlsson, R. Jansson, R. Marcilla, M. Hedhammar, O. Inganas, *Adv. Mater.* **2011**, *23*, 898.

[13] a) D. De Rossi, *Nat. Mater.* **2007**, *6*, 328; b) M. Stoppa, A. Chiolerio, *Sensors* **2014**, *14*, 11957.

[14] M. Hamedi, L. Herlogsson, X. Crispin, R. Marcilla, M. Berggren, O. Inganäs, *Adv. Mater.* **2009**, *21*, 573.

[15] C. J. Park, J. S. Heo, K.-T. Kim, G. Yi, J. Kang, J. S. Park, Y.-H. Kim, S. K. Park, *RSC Adv.* **2016**, *6*, 18596.

[16] G. Tarabella, M. Villani, D. Calestani, R. Mosca, S. Iannotta, A. Zappettini, N. Coppede, *J. Mater. Chem.* **2012**, *22*, 23830.

[17] N. Coppede, G. Tarabella, M. Villani, D. Calestani, S. Iannotta, A. Zappettini, *J. Mater. Chem. B* **2014**, *2*, 5620.

[18] http://www.teleflexmedicaloem.com/suture-and-fiber-technologies/nylon/ (accessed: April 2018).

[19] a) L. Zhang, M. Baima, T. L. Andrew, *ACS Appl. Mater. Interfaces* **2017**, *9*, 32299; b) L. Zhang, M. Fairbanks, T. L. Andrew, *Adv. Funct. Mater.* **2017**, *27*, 1700415.

[20] a) J. Rivnay, P. Leleux, M. Sessolo, D. Khodagholy, T. Herve, M. Fiocchi, G. G. Malliaras, *Adv. Mater.* **2013**, *25*, 7010; b) O. Yaghmazadeh, F. Cicoira, D. A. Bernards, S. Y. Yang, Y. Bonnassieux, G. G. Malliaras, *J. Polym. Sci., Part B:Polym. Phys.* **2011**, *49*, 34.

[21] N. D. Robinson, P.-O. Svensson, D. Nilsson, M. Berggren, *J. Electrochem. Soc.* **2006**, *153*, H39.

[22] L. Zhang, T. L. Andrew, *Adv. Mater. Interfaces* **2017**, *4*, 1700873.

